

# Reversible modulation and ultrafast dynamics of THz resonances in strongly photoexcited metamaterials

I. Chatzakis,<sup>1</sup> L. Luo,<sup>1</sup> J. Wang,<sup>1,†</sup> N-H. Shen,<sup>1</sup> T. Koschny,<sup>1</sup> J. Zhou,<sup>2,‡</sup> and C. M. Soukoulis<sup>1,3</sup>

<sup>1</sup>*Ames Laboratory and Department of Physics and Astronomy,  
Iowa State University, Ames, Iowa 50011, U.S.A.*

<sup>2</sup>*Center for integrated Nanotechnologies, Los Alamos National Laboratory, Los Alamos, New Mexico 87545, USA.*

<sup>3</sup>*Institute of Electronic Structure and Laser, FORTH, 71110 Heraklion, Crete, Greece*

(Dated: December 30, 2011)

We demonstrate an ultrafast reversible modulation of resonant terahertz (THz) response in *strongly photoexcited* metamaterials. The transient spectral-temporal response of the dipole transition  $\sim 1.6$  THz exhibits a distinct non-monotonic variation as a function of pump fluence. The transition energy shift, strength, spectral width and density-dependent ultrafast relaxation manifest a remarkable re-emergence of the resonances after initial quenching. Our simulation, incorporating the first-order diffraction from the photoinduced transient grating, reproduces the salient features, providing a new avenue for designing nonlinear and frequency-agile THz modulators.

PACS numbers: 78.67.Pt, 78.20.-e, 78.47.-p, 42.25.Bs

Artificially subwavelength structured materials, so-called metamaterials [1–4], attract strong current interest due to their exceptional properties, such as simultaneously negative permittivity  $\varepsilon(\omega)$  and permeability  $\mu(\omega)$ , which implies a negative refractive index [1–5] not available in natural materials. In addition, artificial magnetism [6, 7], super focusing [8, 9] and specifically tailored structures responding to ultra-broadband electromagnetic radiation, from gigahertz (GHz), terahertz (THz) to visible range [4, 10], set them among the most promising candidates for next generation optoelectronic devices and large-scale photonic functional systems.

Recently, there has been significant interest in understanding ultrafast THz responses of nonlinear metamaterials, e.g., split ring resonators (SRRs) patterned on substrates exhibiting substantial nonlinearities [11]. The resulting components and schemes allow for constructing controllable active THz devices with dynamical tunability of amplitude and phase, which fills the demanding THz technology gap. Prior experiments using time-domain THz spectroscopy have demonstrated dynamic tuning of both magnetic [12–17] and electric [18] dipole resonances of SRRs on semiconductors or superconductors. More complex structures of coupled resonators on GaAs substrates have been proposed and experimentally studied, revealing frequency-agile THz modulation, e.g., a resonance shift with increasing photoexcitation [14, 16]. However, thus far all ultrafast studies of THz materials have been concentrated on the relatively low photoexcitation, where a *reduction* or *quenching* of the resonant absorptions is observed [13, 14, 19]. Two outstanding issues are still poorly understood: first, there lack insights on how *high density* photoexcited carriers modify the dynamic responses of metamaterials; second, the decay pathway of photoexcited metamaterials after femtosecond (fs) excitation is not explicitly studied, and, particularly, the temporal evolution of the transient states

have only been understood as a density-*independent* relaxation back to the equilibrium.

In this letter, we demonstrate an ultrafast reversible modulation of resonant THz absorption in *strongly photoexcited* metamaterials by optical pump and THz probe spectroscopy. This process directly manifests itself via a remarkable reemergence of the originally quenched THz resonance above a crossover density  $N_c \sim 4.7 \times 10^{16} \text{ cm}^{-3}$  after femtosecond photo-excitation. Increasing the excitation from below to above the transition density, we identify two distinctly different relaxation pathways of the THz resonance with opposite dynamics. A model calculation of transient spectra incorporating the first order diffraction mode from the photoinduced transient grating reproduces the salient features, which is further corroborated by their dependence on the unit cell lattice constant. The revealed scheme represents a relatively simple and generic approach to achieve nonlinear and frequency-agile functions in THz device without particularly complex structures.

The samples used are double SRRs on GaAs, illustrated in the inset of Fig. 1 (a), which are patterned  $6 \mu\text{m}$  copper rings on high resistivity GaAs of  $630 \mu\text{m}$  thick. We mainly focus on two SRR samples with unit cell lattice constant of  $50 \mu\text{m}$  and  $45 \mu\text{m}$ , and the outer dimension of an individual SRR is  $36 \mu\text{m}$ . Our optical pump and THz probe spectroscopy setup is driven by a 1 kHz Ti:sapphire regenerative amplifier with 40 fs pulse duration at 800 nm. One part of the output is used to excite the sample, while a small fraction is used to generate and detect THz pulses [20]. Phase-locked THz field transients are used as a probe, which is generated via optical rectification and detected by electro-optic sampling in 1 mm ZnTe crystals (supplementary material). Copper apertures of 2.5 mm are placed in front of the sample and a GaAs reference to ensure a uniform illumination and faithful comparison. The THz field transmis-

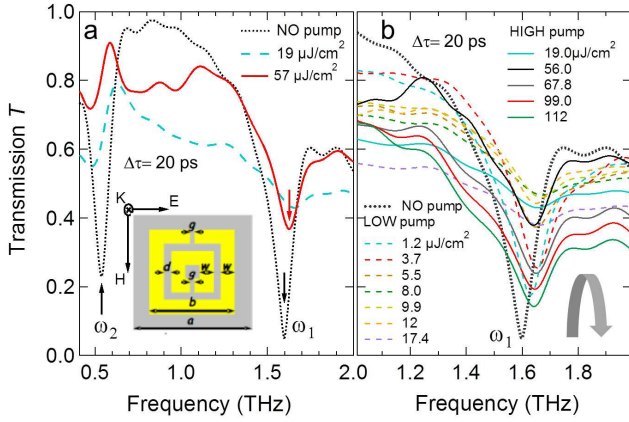


FIG. 1. (color online)(a): Transient transmission spectra  $T(\omega)$  taken under two excitation fluences,  $19 \mu\text{J}/\text{cm}^2$  (cyan dashed) and  $57 \mu\text{J}/\text{cm}^2$  (red solid), respectively. Static transmission spectra without pump is plot together (black dotted). The inset: the SRR unit cell of our sample and the polarization of the normally incident THz radiation.  $a=50 \mu\text{m}$ ,  $b=36 \mu\text{m}$ ,  $d=3 \mu\text{m}$ ,  $g=2 \mu\text{m}$  and  $w=6 \mu\text{m}$ . (b): The non-monotonic pump fluence dependence (indicated by the gray arrow) of the resonant absorption  $\sim 1.63$  THz for low (dashed lines) and high (solid lines) photoexcitation. Spectra In both panels are taken at fixed time delay of  $20 \text{ ps}$ .

sion coefficient  $T(\omega)$  is obtained by the ratio between two Fourier transformed spectra from the transmitted THz probe pulses through the SRRs and bare GaAs. The transient THz signals are recorded at various time delays with respect to the pump pulse to obtain time-dependent  $T(\omega)$ . The whole setup is purged with dry-N<sub>2</sub> gas.

The static transmission spectra are shown in Fig. 1(a) (black dotted) with a THz probe normally incident on the sample plane. The  $E$  field of the probe is parallel to the gaps of SRRs (inset). There are two main THz resonances detected in this configuration at  $\omega_1 \sim 1.6$  THz and  $\omega_2 \sim 0.5$  THz, which originate from resonant electric processes consistent with the prior measurements [13, 18]. The  $\omega_1$  can be understood as the electric dipole resonance of the metallic bars of the SRRs, and the  $\omega_2$  is the magnetic dipole resonance induced by the circulating electric currents generated by the incident  $E$  field.

The two THz resonances exhibit distinctly different pump fluence dependence, as shown in the transient THz transmission spectra at  $\Delta\tau = 20 \text{ ps}$  (Fig. 1(a)) for two pump fluences:  $19 \mu\text{J}/\text{cm}^2$  (cyan dashed) and  $56 \mu\text{J}/\text{cm}^2$  (red solid). The  $20 \text{ ps}$  time-delay between the excitation and probe pulse is introduced to ensure a measure of quasi-steady state considering the transient carrier lifetime in GaAs on the order of  $1 \text{ ns}$ . The  $19 \mu\text{J}/\text{cm}^2$  trace exhibits largely quenched resonances for both the  $\omega_1$  and  $\omega_2$  after the photoexcitation. However, the  $56 \mu\text{J}/\text{cm}^2$  trace clearly shows substantial recovery of the resonant THz absorption around  $\omega_1$ , while the  $\omega_2$  resonance re-

mains quenched. This salient feature is further corroborated in the detailed pump fluence dependence shown in Fig. 1(b). In the low excitation regime from  $1.2$  to  $19 \mu\text{J}/\text{cm}^2$ , there is a clear weakening in the transition strength and broadening in the linewidth for the  $\omega_1$  resonance, with an almost complete quenching at pump fluence of  $19 \mu\text{J}/\text{cm}^2$ . Here the transmission is  $\sim 45\%$  higher and the peak energy has a blue shift of  $\sim 60 \text{ GHz}$ . In strong contrast to this, further increasing photoexcitation from  $56 \mu\text{J}/\text{cm}^2$  to  $112 \mu\text{J}/\text{cm}^2$  results in a progressively pronounced resonance. The spectra clearly show a red shift of the resonance energy,  $\sim 20 \text{ GHz}$  for the highest pump fluence used, a partial recovery of the transition strength and linewidth narrowing. This remarkable non-monotonic behavior and re-emerging resonance near the  $\omega_1$  manifest a reversible and frequency-agile modulation of the resonant THz absorption by photoexcitation. This behavior has been seen experimentally for the first time, and we can explain below that for very high pump fluence the first-order diffraction will surpass the electric resonance behavior in the THz responses of photoexcited metamaterials. Fig. 1(b), the dips in the transmission above  $56 \mu\text{J}/\text{cm}^2$  are due to the first-order diffraction peaks, which will be discussed further below.

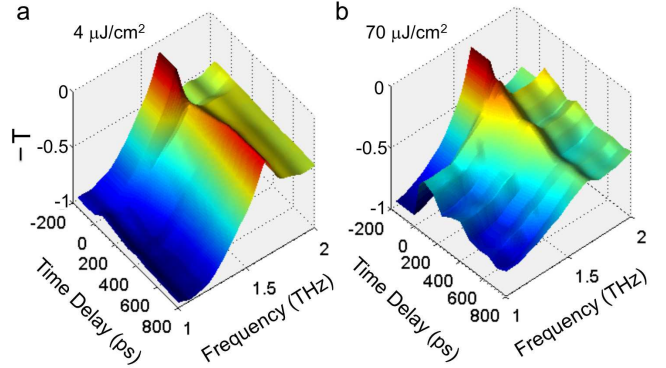


FIG. 2. (color online) Time evolution of negative transmission spectra,  $-T(\omega)$ , in the photoexcited metamaterial of  $50 \mu\text{m}$  lattice constant for (a)  $4 \mu\text{J}/\text{cm}^2$  and (b)  $70 \mu\text{J}/\text{cm}^2$ , respectively. These clearly show the opposite relaxation pathways for the weak and strong excitation regimes (see text).

The weak and strong photoexcitations lead to significantly different relaxation pathways back to the equilibrium, as shown in the time evolution of  $T(\omega)$  spectra following photoexcitation in Figs. 2(a) and 2(b). For pump fluence at  $4 \mu\text{J}/\text{cm}^2$ , the THz absorption  $\sim \omega_1$  resonance exhibit an initial photoinduced reduction, immediately followed by a relaxation back to the original value on a  $\text{ns}$  time scale. Interestingly enough, opposite to those at the low excitation, the  $70 \mu\text{J}/\text{cm}^2$  dynamics clearly shows a further reduction of the THz resonance  $\sim 1.6$  THz following the initial decrease. We emphasize two key aspects of this observation: (i) at the large time delay of  $\Delta\tau = 800 \text{ ps}$ , the THz resonance  $\sim 1.6$  THz is almost com-

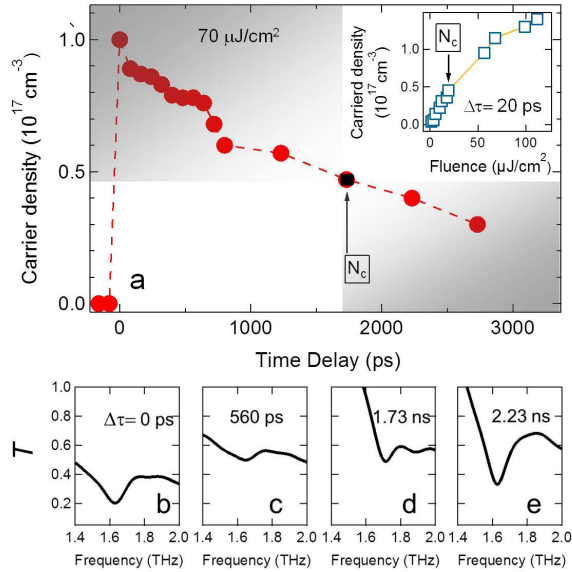


FIG. 3. (color online)(a) The extracted transient carrier concentration as function of time delay. The left and right gray areas illustrate a crossover from the high to low excitation regime with a crossover density  $N_c$  (black square). The inset plots the extracted transient carrier concentration as function of pump fluence at  $\Delta\tau = 20 \text{ ps}$ , marked together with  $N_c$  corresponding to the density excited by  $19 \mu\text{J}/\text{cm}^2$ . (b)-(e): The transient transmission spectra  $T(\omega)$  at various time delays following  $70 \mu\text{J}/\text{cm}^2$  photoexcitation.

pletely quenched for the  $70 \mu\text{J}/\text{cm}^2$  excitation, although a clear recovery of the resonance has been seen for the  $4 \mu\text{J}/\text{cm}^2$  case; (ii) the pump-fluence-dependent relaxation dynamics of the resonance indicates another way to achieve nonlinear and reversible THz modulation by tuning the time delay.

Ultrafast photoexcitation strongly alters the electronic states in GaAs substrate by injecting non-equilibrium transient carriers during the pulse duration of 40 fs. Subsequent carrier-carrier/carrier-phonon collisions lead to decoherence and then to a quasi-thermal, hot transient carrier distribution within 1 ps. This hot carrier distribution further cools down by emitting phonons and eventually relaxes back to the equilibrium by carrier recombination on the order of 1 ns. In the weak excitation regime below  $19 \mu\text{J}/\text{cm}^2$  (see Fig. 1), the injected carriers make the GaAs regions in the gaps of SRRs and in between them conductive. This leads to the reduction of the resonant absorption near  $\omega_1$  and even complete quenching of the resonances [13]. Thus the observed crossover from the photoinduced quenching to re-emergence of the THz resonance clearly indicate a new collective excitation setting in at the high excitation regime, not accessible in the previous measurements.

To gain quantitatively insights into the transition density  $N_c$  for the excitation-induced crossover behavior, we experimentally determine temporal evolution of the tran-

sient carrier density. The phase-sensitive nature of the time-domain THz field measurement can directly yield both real and imaginary parts of the optical conductivity in the photoexcited GaAs substrate, on equal footing without any model assumptions. This gives a direct determination of the transient carrier density based on an analysis using the Drude model (see supplementary material). Figure 3(a) plots the temporal evolution of the transient carrier concentration excited by  $70 \mu\text{J}/\text{cm}^2$ , which shows an exponential decay with a peak density  $10^{17} \text{ cm}^{-3}$ . By correlating the temporal profile to the fluence-dependent carrier concentration at  $\Delta\tau = 20 \text{ ps}$  (inset, Fig. 3(a)), one can define a crossover point at density  $N_c \sim 4.7 \times 10^{16} \text{ cm}^{-3}$  at time delay of  $\Delta\tau_c \sim 1.73 \text{ ns}$  (black square), corresponding to the transient density for  $19 \mu\text{J}/\text{cm}^2$ . This naturally divides the transient electronic response of photoexcited metamaterials into two regimes with opposite time and excitation dependence, as illustrated in the shaded areas of Fig. 3(a). Transient spectra at various time delays, as shown in Figs. 3(b)-(e), show a reversal of the THz transmission change once the system is driven cross the boundary, corroborating well of our conclusion, e.g., the THz transmission recovers its strength at  $\Delta\tau = 2.2 \text{ ns}$  after initial quenching at time delays before 1.73 ns.

Next, we analyze the transient THz response of photoexcited metamaterials by full-wave numerical simulations. Before we take into account any complex processes, we first simply consider the photoexcitation-induced dynamic response of the GaAs substrate beneath the SRRs. A photoexcited layer is modeled by the well-established Drude model, in which, the frequency-dependent complex conductivity  $\sigma = \varepsilon_0 \omega_p^2 / (\gamma - i\omega)$ . Here,  $\varepsilon_0$  is the permittivity of vacuum,  $\gamma$  represents the collision frequency, and  $\omega_p = \sqrt{N e^2 / (\varepsilon_0 m^*)}$  the plasma frequency. Some other parameters include the carrier density  $N$ , the free electron charge  $e$  ( $1.6 \times 10^{-19} \text{ C}$ ) and the effective carrier mass in GaAs,  $m^* = 0.067 m_0$  ( $m_0$ , the mass of a free electron). Thus, the photoexcited layer has the dielectric function  $\varepsilon(\omega) = \varepsilon_s + i\sigma / (\varepsilon_0 \omega)$ , where  $\varepsilon_s$  ( $= 12.7$ ) is the dielectric constant of undoped GaAs. In our simulations, we keep  $\gamma = 1.8 \text{ THz}$  for all the cases as in Ref. 17.

Figure 4(a) shows the simulated transmission spectra for various carrier density  $N$ . The simulation clearly shows the crossover from a reduction to an enhancement of the resonant THz absorption  $\sim 1.6 \text{ THz}$  as the excitation from low to high density regime. This agrees well with the photoinduced reversible modulation demonstrated in the experiments. Specifically, in the low density below  $4.0 \times 10^{16} \text{ cm}^{-3}$ , the THz resonance peak in the transmission curve exhibit clearly weakened transition strength, a blue-shift and spectral broadening. Increasing the carrier density above  $4.0 \times 10^{16} \text{ cm}^{-3}$ , the resonant THz peak progressively reemerges, e.g., a clear transmission dip seen for the case  $N = 8.1 \times 10^{17} \text{ cm}^{-3}$ .

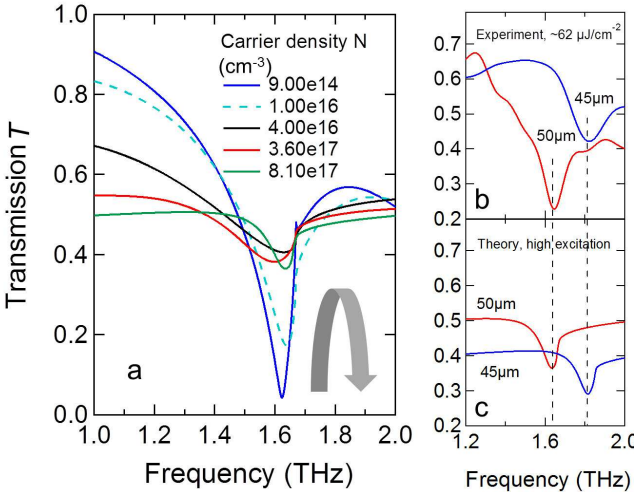


FIG. 4. (color online) (a): The simulated THz transmission spectra for various carrier densities  $N$ . The photoinduced THz resonances in the strong excitation regime for two different lattice constants 45 and 50  $\mu\text{m}$ : (b) experiment and (c) simulation.

From the simulations, we can attribute the reemergence of the resonant THz absorption at high density to the effect of first-order diffractive waves from photoinduced transient grating. Due to the periodic structure of the SRRs, the first-order diffractive wave is found to propagate in the substrate at high excitation, which strongly influence the fundamental absorption mode. This leads to a new THz transmission dip at  $f_1 = c/(na)$  above a transition density  $\sim 4.0 \times 10^{16} \text{ cm}^{-3}$ . Here  $c$  is light speed in vacuum,  $n$  the refractive index of GaAs and  $a$  the lattice constant of the structure. The SRR structure with the dipole resonance close to  $f_1$  allows to achieve a reversal of resonant THz absorption with increasing photoexcitation, due to a crossover in the absorption from the dipole mode to the diffraction mode.

To corroborate our model, we compare the re-emerged THz resonances from the experiment (Fig. 4(b)) to those from the simulation (Fig. 4(c)) for two different lattice constants, 50  $\mu\text{m}$  and 45  $\mu\text{m}$ , respectively. The simulations are performed to the structures with the same double-SRR array for the case with the density  $N = 8.1 \times 10^{17} \text{ cm}^{-3}$ . It is clearly visible that the simulated transmission dip to higher frequency by decreasing the lattice constant, and the dip positions tightly link to the frequency of the first-order diffraction mode for each case. An extremely good agreement between the simulation and the experiment is found for the transmission-dip position and its shift, which underpins the effect of the high-order diffraction mode in the strongly excited metamaterials.

In summary, we have demonstrated ultrafast photoinduced reversible modulation of resonant THz absorption in strongly photoexcited metamaterials. Increasing the

excitation from below to above the threshold density  $N_c$ , we observe a crossover from a complete quenching to a reemergence of the THz resonance. Our analysis and theoretical simulations, based on the first order propagation from the photoinduced transient grating, explain the density- and lattice-constant-dependent frequency shift. Our results clearly identify the importance of photoinduced optical modes in metamaterials, besides the electronic resonances, which should be carefully considered in designing future multifunctioning photonic-electronic devices using the artificial periodical structures. The easy implementation of the revealed scheme represents another approach to achieve nonlinear and frequency-agile functions in THz devices.

Work at Ames Laboratory was supported by the Department of Energy (Basic Energy Sciences) under contract No. DE-AC02-07CH11358. This was partially supported by IC Postdoctoral Fellowship Program.

<sup>†</sup>To whom correspondence should be addressed. Electronic address: jgwang@iastate.edu

<sup>‡</sup>Present address: Department of Physics, University of South Florida, Tampa, FL

---

- [1] D. R. Smith, J. B. Pendry and M. C. K. Wiltshire, *Science* **305**, 788 (2004).
- [2] C. M. Soukoulis, S. Linden, and M. Wegener, *Science* **315**, 47 (2007).
- [3] V. M. Shalaev, *Nature Photon.* **1**, 41 (2007).
- [4] C. M. Soukoulis and M. Wegener, *Nature Photon.* **5**, 523 (2011).
- [5] R. A. Shelby, D. R. Smith, S. Shultz *Science* **7**, 292 (2001).
- [6] T. J. Yen, et al., *Science* **303**, 1494 (2004).
- [7] S. Linden *et al.*, *Science* **306**, 1351 (2004).
- [8] N. Fang, H. Lee, C. Sun, and X. Zhang, *Science* **308**, 534 (2005).
- [9] J. B. Pendry, *Phys. Rev. Lett.* **85**, 3966 (2000).
- [10] S. Zhang *et al.*, *Phys. Rev. Lett.* **95**, 137404 (2005).
- [11] A. K. Azad, J. Dai, and W. Zhang, *Opt. Lett.* **31**, 634 (2006).
- [12] H. T. Chen, W. J. Padilla, J. M. O. Zide, A. C. Gossard, A. J. Taylor, and R. D. Averitt, *Nature* **444**, 597 (2006).
- [13] W. J. Padilla, A. J. Taylor, C. Highstrete, M. Lee, and R. D. Averitt, *Phys. Rev. Lett.* **96**, 107401 (2006).
- [14] N. H. Shen *et al.* *Phys. Rev. Lett.* **106**, 037403 (2011).
- [15] H. T. Chen *et al.*, W. J. Padilla, J. M. O. Zide, S. R. Bank, A. C. Gossard, A. J. Taylor, and R. D. Averitt, *Opt. Lett.* **32**, 1620 (2007).
- [16] H. T. Chen *et al.*, J. F. O'Hara, A. K. Azad, A. J. Taylor, R. D. Averitt, D. B. Shrekenhamer, and W. J. Padilla, *Nature Photon.* **2**, 295 (2008).
- [17] H. T. Chen *et al.*, *Phys. Rev. Lett.* **105**, 247402 (2011).
- [18] J. M. Manceau, N. H. Shen, M. Kafesaki, C. M. Soukoulis, and S. Tzortzakis, *Appl. Phys. Lett.* **96**, 021111 (2010).
- [19] K. M. Dani *et al.*, *Nano Lett.* **9**, 3565 (2009).
- [20] Q. Wu and X.-C. Zhang, *Appl. Phys. Lett.* **68**, 1604 (1996).